Proceedings of the CAS–CERN Accelerator School: Free Electron Lasers and Energy Recovery Linacs, Hamburg, Germany, 31 May–10 June 2016, edited by R. Bailey, CERN Yellow Reports: School Proceedings, Vol. 1/2018, CERN-2018-001-SP (CERN, Geneva, 2018)

Motion in the Undulator

S. Reiche
Paul Scherrer Institute, Villigen, Switzerland

Abstract
This paper gives an introduction to the theoretical framework for the motion of an electron in the periodic field of an undulator and wiggler. The equations of motion are derived and solved for planar and helical devices.

Keywords
Free-electron laser; theory; undulator; electron motion.

1 Electron motion in an undulator or wiggler

The hardware part of a free-electron laser is an undulator or wiggler. Its main purpose of the undulator or wiggler is to force the electrons to oscillate ('wiggle') as they move through it. This transverse motion causes the electron beam to emit synchrotron radiation. For relativistic electrons, the synchrotron radiation is confined to a forward cone. The opening angle is the inverse of the Lorentz factor $\gamma = E/mc^2$, where E is the electron energy, m is the electron mass, and c is the speed of light.

The main feature of an undulator and wiggler is a series of paired magnets along the main axis. They are placed opposite to each other, separated by a gap of width g. The magnetic flux has only a component transverse to the undulator axis. If the plane of the gap is fixed, the undulator or wiggler is planar. Another type of undulator involves rotation of the magnets along the main axis, in the form of a double helix. This type of undulator is called helical.

A Cartesian co-ordinate system, where the z-axis coincides with the undulator axis, will be used throughout this paper. The transverse co-ordinates x and y are chosen so that the magnetic field for a planar undulator or wiggler is parallel with the y-axis. Owing to rotational symmetry, the choice of co-ordinate system orientation for the helical undulator is arbitrary. Here, it is defined so that the magnetic field at the undulator entrance ($z = 0$) has only field components in the y-direction.

A higher magnetic field strength can be achieved by hybrid magnets, in which iron poles with high permeability are placed between permanent magnets [1]. Figure 1 shows a schematic cross-section of a planar undulator or wiggler based on hybrid magnets. The magnetic field of the permanent magnets points in either the positive or negative z-direction. The flux of two adjoining magnets is bent into the transverse direction by the iron pole. The advantage of this method is that the cross-section of the iron pole faces is smaller than that of the permanent magnets themselves. Therefore, the maximum achievable magnetic field can be increased by compressing the magnetic flux. A magnetic field strength larger than 2 T can then be obtained.

Wigglers and undulators differ in the deflection strength of the magnetic field. If the maximum deflection angle is larger than the opening angle of the spontaneous emission, there is no continuous emission in the forward direction, resulting in a wiggler. The spectrum observed is enriched by higher harmonics of the periodic signal of the detected radiation. Undulator radiation is modulated but not pulsed in the forward direction and the number of higher harmonics in the spectrum is reduced. A typical spectrum for the TESLA Test Facility is shown in Fig. 2. A more quantitative criterion to distinguish undulators and wigglers is given later in this section. Although both undulators and wigglers are used for free-electron lasers, for the sake of simplicity, the remaining part of this paper refers only to undulators, unless necessity requires that the two types must be distinguished.

https://doi.org/10.23730/CYRSP-2018-001.347

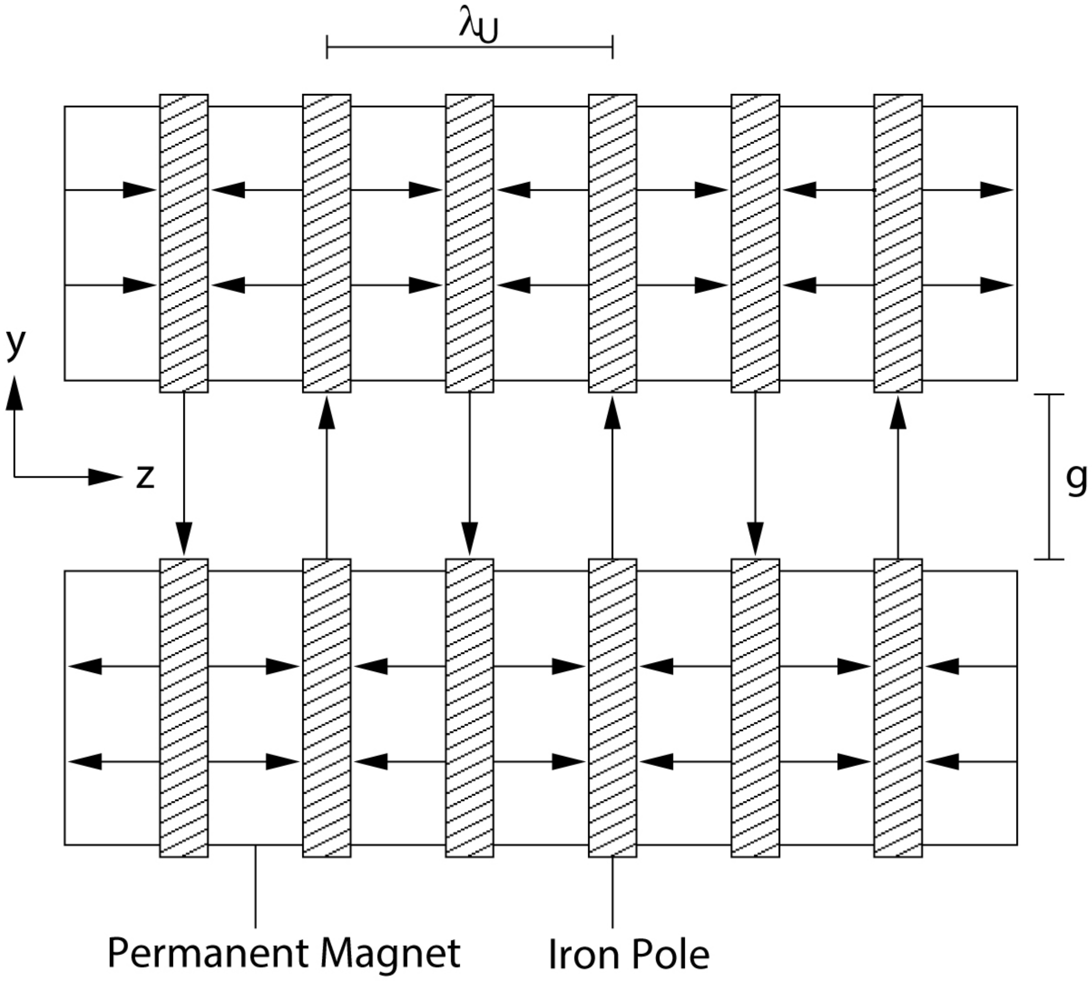

Fig. 1: Cross-section of planar undulator with gap width g and periodicity λ_U. The direction of the magnetic field is indicated by arrows.

1.1 The planar undulator

The discussion begins with the derivation of the electron trajectories within the planar undulator. The calculation for the helical case is similar and is given in the next subsection in a more compressed form.

The magnetic field at the undulator axis is a harmonic function of the longitudinal position z:

$$B_y(z, x = 0, y = 0) = B_0 \cos(k_U z) \,.$$

The field points in the y-direction and has an amplitude B_0 and a wavenumber $k_U = 2\pi/\lambda_U$. Although it might be desirable, the field cannot be constant over the whole transverse plane. Within the free space of the undulator gap, Maxwell's equations for a static magnetic field require that the divergence and curl vanish ($\vec{\nabla} \cdot \vec{B} = 0$ and $\vec{\nabla} \times \vec{B} = 0$). The second condition determines the dependence of the magnetic field on the transverse co-ordinates. It also allows the magnetic field to be derived from a scalar potential ϕ with $\vec{B} = -\vec{\nabla}\phi$. To fulfil Maxwell's equations, the scalar potential ϕ must be a solution of the Laplace equation $\Delta\phi = 0$.

A good starting assumption is

$$\phi = -\frac{B_0}{k_y} \cosh(k_x x) \sinh(k_y y) \cos(k_U z) \,, \tag{1}$$

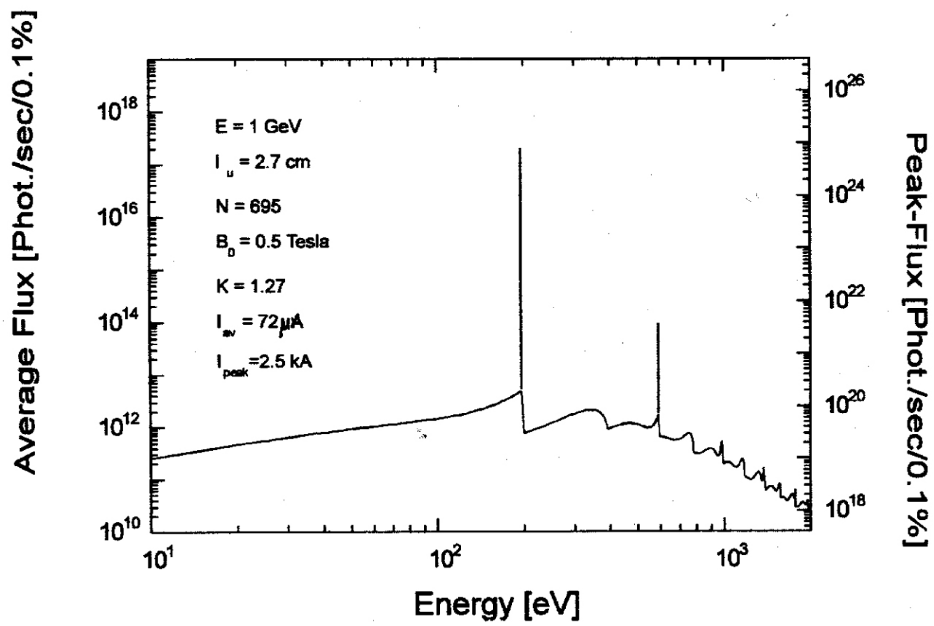

Fig. 2: Radiation spectrum of the free-electron laser at the TESLA Test Facility

which gives the desired magnetic field at the axis. Inserting Eq. (1) into the Laplace equation, the scalar potential is a physically reasonable solution if the relation

$$k_x^2 + k_y^2 = k_U^2 \tag{2}$$

is valid [2]. In general, to a good approximation, a magnetic field is perpendicular to the pole faces. This implies that the pole faces can be identified with equipotential surfaces, where the scalar potential ϕ is constant. For any arbitrarily chosen position z, the curvature of the equipotential surface is defined by the relation $\cosh(k_x x)\sinh(k_y y) =$ constant. It can be seen that y must be constant for $k_x = 0$ and that the pole faces are plane. The case of an outward bent pole face is covered by an imaginary value of k_x or, which is equivalent, by replacing the cosh function in Eq. (1) with the cosine function. In this case, k_y^2 becomes larger than k_U^2. For real values of k_x with $k_x > 0$, the two opposite poles are bent towards each other and k_y is either reduced ($k_x < k_U$), zero ($k_x = k_U$), or imaginary ($k_x > k_U$).

For x and y small compared with the undulator period length, so that $k_x x, k_y y \ll 1$, the hyperbolic function can be expanded into a Taylor series up to the second order. In this approximation, which is reasonable for most undulators up to a beam radius of typically 1 mm, the magnetic field becomes

$$\vec{B} = B_0 \begin{pmatrix} k_x^2 xy\cos(k_U z) \\ \left(1 + \frac{k_x^2 x^2}{2} + \frac{k_y^2 y^2}{2}\right)\cos(k_U z) \\ -k_U y \sin(k_U z) \end{pmatrix} . \tag{3}$$

The extra field caused by the curved pole faces is equivalent to a sextupole field with amplitude $B_0 k_x^2$. As shown later in this section, it provides focusing of the electron beam in the x-direction.

For further discussion, it is useful to know the vector potential $\vec{A}$ of the undulator field. This is given by

$$\vec{A} = \frac{B_0}{k_U} \begin{pmatrix} \left(1 + \frac{k_x^2}{2}x^2 + \frac{k_y^2}{2}y^2\right)\sin(k_U z) \\ -k_x^2 xy\sin(k_U z) \\ 0 \end{pmatrix} , \tag{4}$$

with $\vec{B} = \vec{\nabla} \times \vec{A}$.

The equations of motion for the position $\vec{r}$ and canonical momentum $\vec{P}$ of a single electron [3] are obtained from the Hamilton formalism, using the Hamilton function of a relativistic electron,

$$H = \sqrt{(\vec{P} - e\vec{A})^2 c^2 + m^2 c^4} + e\Phi\,, \tag{5}$$

where Φ is the scalar potential of the electric field $\vec{E}$ with $\vec{E} = -\vec{\nabla}\Phi - \partial\vec{A}/\partial t$.

If the electron is relativistic with $\gamma \gg 1$, the motion of the electron is mainly defined by the magnetic field of the undulator. Interaction with a radiation or electrostatic field can be regarded as a perturbation. These effects, which are important for the free-electron lasing process, are discussed in later sections.

With this assumption, the Hamilton function is a constant of motion because it does not depend explicitly on the time t. Owing to the absence of an electric field ($\Phi = 0$), the electron energy γmc^2 is also constant and identical in value to the Hamilton function.

It is difficult to solve the equations of motion directly. Therefore, the electron motion is split into two parts,

$$\vec{r}(t) = \vec{r}_0(t) + \vec{R}(t)\,,$$

separating the main oscillation $\vec{r}_0(t)$ due to the periodic undulator field from a drift $\vec{R}(t)$ in the transverse position. The drift is slow compared with the quickly varying term $\vec{r}_0(t)$ and has a characteristic length of the scale of many undulator periods. As a first step, the solution for $\vec{r}_0$ is obtained by assuming that $\vec{R}(t)$ is constant.

The equations of motion for the transverse canonical momentum $\vec{P}$ are

$$\dot{P}_x = -\frac{\partial}{\partial x}H = \frac{e}{\gamma m}\left(\frac{\partial}{\partial x}\vec{A}\right)\cdot\left(\vec{P} - e\vec{A}\right)\,, \tag{6}$$

$$\dot{P}_y = -\frac{\partial}{\partial y}H = \frac{e}{\gamma m}\left(\frac{\partial}{\partial y}\vec{A}\right)\cdot\left(\vec{P} - e\vec{A}\right)\,. \tag{7}$$

For the vector potential of Eq. (4), the lowest-order term of the time derivative $\dot{\vec{P}}$ is linear in $k_x x$ or $k_y y$, respectively. As mentioned at the expansion of the hyperbolic function in Eq. (3), these linear terms are small compared with unity. Thus, the change in the canonical momentum contributes either to the ‘slow’ motion $\vec{R}(t)$ or to the higher-order solutions of $\vec{r}_0$, which are not regarded in this discussion.

The remaining equations of the transverse motion,

$$\dot{x} = \frac{\partial}{\partial P_x}H = \frac{P_x - eA_x}{\gamma m}\,, \tag{8}$$

$$\dot{y} = \frac{\partial}{\partial P_y}H = \frac{P_y - eA_y}{\gamma m}\,, \tag{9}$$

have only one dominant and quickly oscillating source term, given by the x-component of the vector potential in Eq. (8). The resulting motion takes place in the xz-plane with the ‘fast’ velocity

$$\dot{x}_0 = -\frac{\sqrt{2}cK}{\gamma}\sin(k_U z)\,. \tag{10}$$

Equation (10) suggests the definition of the dimensionless undulator field:

$$K = \frac{e\hat{B}}{mck_U}\left(1 + \frac{k_x^2}{2}X^2 + \frac{k_y^2}{2}Y^2\right)\,, \tag{11}$$

depending, to second order, on the transverse position $X = X(t)$ and $Y = Y(t)$ of the ‘slow’ trajectory $\vec{R}(t)$. This definition differs from that given in other publications, where the on-axis peak field B_0 is used instead of the r.m.s. value $\hat{B}$. In the case of a planar undulator, $\hat{B}$ is $B_0/\sqrt{2}$. The advantage of this definition is that many equations remain the same for the case of the helical undulator. The value of K at the undulator axis ($X, Y = 0$) defines the undulator parameter. Because the second-order corrections to the undulator field are of the order of 10^{-3}, the transverse dependence of the undulator field has a negligible impact on most of the calculations. Therefore, it is sufficient to use the constant value of the undulator parameter instead.

Equation (10) exhibits the distinction between a wiggler and an undulator. If the electron is relativistic ($z \approx ct$), the maximum divergence $x' = \dot{x}_0/c$ of the electron is $\sqrt{2}K/\gamma$. The opening angle of the synchrotron radiation is γ^{-1}; thus, the device is an undulator for $K \leq 1/\sqrt{2}$ and a wiggler otherwise.

There is no dominant component of the vector potential in y and the motion in this direction consists only of the 'slow' motion ($y_0(t) = 0$).

Owing to energy conservation, the longitudinal velocity can be obtained directly from the definition of the Lorentz factor γ and the normalized velocity $\vec{\beta} = \mathrm{d}\vec{r}/c\mathrm{d}t$. Then the longitudinal velocity is

$$
\begin{aligned}
\beta_z &= \sqrt{1 - \frac{1}{\gamma^2} - \beta_x^2 - \beta_y^2} \\
&\approx 1 - \frac{1+K^2}{2\gamma^2} - \frac{\beta_R^2}{2} + \frac{K^2}{2\gamma^2}\cos(2k_U z)\,,
\end{aligned}
\tag{12}
$$

where β_R is the transverse velocity of the slow drift, normalized to c. The cross term proportional to $\beta_R K/\gamma \cdot \sin(k_U z)$ has been neglected because it is either small compared with the leading oscillating term ($\propto K^2 \cos(2k_U z)$) or not resonant with variation of β_z, as is the case for $\beta_R^2/2$.

The transverse motion within the undulator slows down the electron by roughly $\Delta\beta_z = K^2/2\gamma^2$ with a superimposed longitudinal oscillation with a period half as long as the transverse oscillation.

To obtain the trajectory $x_0(t)$, the longitudinal position is approximated by $z = c\beta_z t \approx c\beta_0 t$ and then Eq. (10) is integrated in first order, using the averaged velocity

$$
\beta_0 = 1 - \frac{1+K^2}{2\gamma^2}\,. \tag{13}
$$

The integration yields

$$
x_0(t) = \frac{\sqrt{2}K}{\gamma k_U \beta_0}\cos(ck_U\beta_z t)\,. \tag{14}
$$

The longitudinal oscillating term in Eq. (12) is the source of a phase modulation in the cosine function in Eq. (14). As a consequence, the transverse oscillation exhibits higher harmonics of the fundamental wavenumber k_U. In addition, the synchronization of the electron position with a phase front of an electromagnetic wave, propagating along the undulator axis, is reduced. The impact of both facts will be discussed in the next section. Only slowly varying terms in the equations of motion can contribute to $\vec{R}$. By averaging over one undulator period, Eqs. (8) and (9) are reduced to $\dot{X} = P_x/\gamma m$ and $\dot{Y} = P_y/\gamma m$. The vector potential $\vec{A}$ has only terms proportional to $\sin(k_U z)$ or $\sin(2k_U z)$ and these vanish after averaging. In the remaining equations, Eqs. (6) and (7), all terms are zero except for $(\partial A_x/\partial x)A_x$ and $(\partial A_x/\partial y)A_x$, respectively.

The resulting differential equations

$$
\dot{P}_x = -\gamma mc^2 \frac{K^2 k_x^2}{\gamma^2} X\,, \tag{15}
$$

$$
\dot{P}_y = -\gamma mc^2 \frac{K^2 k_y^2}{\gamma^2} Y\,, \tag{16}
$$

describe reaction forces proportional to the displacement.

The magnetic field of the undulator provides a natural focusing of the electrons if the pole faces are flat or bent towards each other ($k_x^2 \leq 0$). Although the focusing strength in both planes depends on the curvature of the magnetic poles, the combined strength $K^2 k_U^2/\gamma^2$ does not, owing to Eq. (2). For flat horizontal pole faces, there is no focusing in the x-plane. Increasing the focusing strength in this plane involves a reduction in the y-plane. A more precise calculation shows that the finite width of the undulator magnets introduces a small change in the magnetic field, so that a slight defocusing term is noticeable in the x-direction for $k_x = 0$ [4].

The trajectories of the transverse slow motion are harmonic functions with frequencies $\Omega_x = Kk_x/\gamma$ and $\Omega_y = Kk_y/\gamma$, for the x- and y-planes, respectively. The period length λ_β is typically of the order $\lambda_\beta \approx (\gamma/K)\lambda_U$ and thus much larger than the undulator period for a highly relativistic electron ($\gamma \gg 1$). The index β refers to the definitions used in accelerator physics, where this oscillation is called a betatron oscillation [5].

The transverse beam size is strongly related to the focusing strength. The calculations for the y-direction are identical to those for the x-direction, which are presented here. The general betatron oscillation of a single electron is given by $X(t) = X_0 \cos(\Omega_x z) + (X_0'/\Omega_x)\sin(\Omega_x z)$, where X_0 is the initial offset of the electron and X_0' is the initial angle relative to the undulator axis.

The emittance

$$\epsilon_x = \sqrt{\overline{(x-\overline{x})^2}\;\overline{(x'-\overline{x'})^2} - \overline{(x-\overline{x})(x'-\overline{x'})}^2}\,, \tag{17}$$

where a bar over a parameter denotes an average over all electrons, is a constant of motion in linear optics [6]. Regarding this definition of the emittance, $\pi\epsilon_x$ can be identified as an equivalent volume of the electron distribution in the transverse (x, x') phase space.

In contrast with the emittance, the r.m.sq. envelope of the electron beam is usually not a constant of motion [5]. The general expression of the envelope $\sigma_x(z)$ for $k_x^2 > 0$ within an undulator is

$$\sigma_x(z) = \sqrt{\sigma_x(0)^2\cos^2(\Omega_x z) + \frac{\sigma_x(0)\sigma_x'(0)}{2\Omega_x}\sin(2\Omega_x z) + \frac{\epsilon_x^2 - \sigma_x^2(0)\sigma_x'^2(0)}{\sigma_x^2(0)\Omega_x^2}\sin^2(\Omega_x z)}\,, \tag{18}$$

where $\sigma_x(0)$ and $\sigma_x'(0)$ are the initial beam size and its derivative in z, respectively. For a matched beam, when the beam size remains constant over the full undulator length, the electron beam must go through a waist directly at the entrance of the undulator ($\sigma_x'(0) = 0$) with an r.m.s. size of $\sigma_x(0) = \sqrt{\epsilon_x/\Omega_x}$. If the undulator focuses equally in both planes with $k_x = k_U/\sqrt{2}$, the constant size is

$$\sigma_x(0) = \sqrt{(\sqrt{2}mc/e)\epsilon_x\gamma/\hat{B}}\,.$$

All other initial settings cause a modulation of the envelope. If a smaller beam size is desired, it can be achieved by superimposing a lattice of quadrupoles. Normally, this is referred to as strong focusing, in contrast with the natural or weak focusing given by the undulator field itself.

1.2 The helical undulator

The treatment of the helical undulator is very similar to that of the planar one. Indeed most of the results are the same. The magnetic field $\vec{B}$, as well as the vector potential $\vec{A}$, consists of a linear combination of the first-order modified Bessel functions I_0 and I_1 [7], depending only on $k_U r$, where r is the transverse distance between the electron position and the undulator axis. Using the assumption that $k_U r$ is much smaller than unity, the Bessel functions are expanded into a Taylor series. Up to second order in $k_U r$, the vector potential in the Cartesian co-ordinate system is given by

$$\vec{A} = \frac{B_0}{k_U}\begin{pmatrix} \left[1 + \frac{k_U^2}{8}(3y^2 + x^2)\right]\sin(k_U z) - \frac{k_U^2}{4}xy\cos(k_U z) \\ \left[1 + \frac{k_U^2}{8}(3x^2 + y^2)\right]\cos(k_U z) - \frac{k_U^2}{4}xy\sin(k_U z) \\ 0 \end{pmatrix}. \tag{19}$$

The magnetic field is derived in the usual way by evaluating $\vec{B} = \vec{\nabla} \times \vec{A}$.

The trajectory is split into a quickly oscillating term $\vec{r}_0(t)$ and the slow betatron oscillation $\vec{R}(t)$. The velocity of the fast motion $\dot{\vec{r}}_0$ is proportional to the vector potential. Close to the undulator axis, $\dot{x}_0$ and $\dot{y}_0$ have the same amplitude of oscillation but they have a phase difference of $\pi/2$. This is an obvious result, which can be expected because of the symmetry of a helical undulator. Off-axis, the velocity differs in both directions, owing to the higher-order terms in x and y of the vector potential. The transverse motion of the electron becomes more elliptical, with the short axis pointing in the radial direction. To eliminate this azimuthal dependence, and for a better comparison with the results for the planar undulator, the vector potential is averaged in the azimuthal direction.

The normalized longitudinal velocity is

$$\beta_z \approx 1 - \frac{1+K^2}{2\gamma^2} - \frac{\beta_R^2}{2}\,, \tag{20}$$

with the undulator field

$$K = \frac{e\hat{B}}{mck_U}\left(1 + \frac{k_U^2}{4}(X^2+Y^2)\right) \tag{21}$$

in the Taylor series expansion up to second order in X and Y.

The major difference between helical and planar undulators becomes apparent here. Because the electron oscillates in both transverse directions but with a $\pi/2$ phase difference, the longitudinal velocity is almost constant. The terms proportional to $\beta_R\cos(k_U z)$ or $\beta_R\sin(k_U z)$ are negligible and not included in Eq. (20). The absence of a longitudinal oscillation excludes the generation of higher harmonics in the transverse motion of the electron. The helical undulator field of Eq. (21) agrees with that of a planar undulator (Eq. (11)) if the planar undulator provides equal focusing in both planes, with $k_x^2 = k_y^2 = k_u^2/2$. This similarity is an advantage of the undulator field definition based on the r.m.s. value $\hat{B}$.

With the definition of β_0 in analogy with Eq. (13), the transverse velocity can be integrated to obtain the trajectory $\vec{r}_0$. The electrons move along a helix with a pitch of λ_U. Owing to the asymmetry in the azimuthal and radial motion for larger transverse offsets, the helix is slightly distorted [8]. The average radius of the motion is independent of the azimuthal angle, with

$$r_0 = \frac{K}{\gamma k_U \beta_0}\,. \tag{22}$$

By averaging the transverse equations of motion over the length of one period, the fast oscillation drops out. Some basic algebra yields the differential equations:

$$\dot{X} = \frac{P_x}{\gamma m} - c\frac{\Omega_U^2}{k_U}Y\,, \tag{23}$$

$$\dot{P}_x = -\gamma mc^2\Omega_U^2 X - c\frac{\Omega_U^2}{k_U}P_y\,, \tag{24}$$

$$\dot{Y} = \frac{P_y}{\gamma m} - c\frac{\Omega_U^2}{k_U}X\,, \tag{25}$$

$$\dot{P}_y = -\gamma mc^2\Omega_U^2 Y - c\frac{\Omega_U^2}{k_U}P_x\,, \tag{26}$$

with $\Omega_U = Kk_u/\sqrt{2}\gamma$.

These differential equations describe two coupled oscillations but they can be decoupled into ordinary differential equations for harmonic oscillations with the frequencies

$$\hat{\Omega} = \Omega_U\left(\sqrt{1+\frac{\Omega_U^2}{k_U^2}} \pm \frac{\Omega_U}{k_U}\right)\,, \tag{27}$$

by transforming to the variables $X \pm \mathrm{i}Y$. The ratio Ω_U/k_U is of the order $1/\gamma$. The characteristic length of the orbit beat by the coupling is roughly $\gamma^2\lambda_U$ and, even for moderately relativistic electrons, much longer than the undulator length itself. This term is only important for storage-ring-based undulators because it is a major source of coupling of the betatron motion [8]. By neglecting the coupling term, Eqs. (23)–(26) become identical to the corresponding equations for the planar undulator, with $k_x^2 = k_y^2 = k_U^2/2$. The conditions for optimum matching of the electron beam are also valid for the helical undulator.

References

[1] K. Halbach, *J. Phys. (Paris)* **C1 44** (1983) 211.

[2] E.T. Scharlemann, *J. Appl. Phys.* **58** (1985) 2154. https://doi.org/10.1063/1.335980

[3] H. Goldstein, *Classical Mechanics* (Addison-Wesley, Reading, MA, 1980).

[4] B. Diviacco and P. Walker, *Nucl. Instrum. Methods*, **A292** (1990) 517. https://doi.org/10.1016/0168-9002(90)90409-Y

[5] D.A. Edwards and M.J. Syphers, *An Introduction to the Physics of High Energy Accelerators* (John Wiley and Sons, New York, 1993). https://doi.org/10.1002/9783527617272

[6] K. Wille, *Physik der Teilchenbeschleuniger und Synchrotronstrahlungsquellen* (B.G. Teubner Verlag, Stuttgart, 1992). https://doi.org/10.1007/978-3-663-11850-3

[7] G. Rowlands, J. *Phys. A: Math. Gen.* **13** (1980) 2839. https://doi.org/10.1088/0305-4470/13/8/031

[8] J.P. Blewett and R. Chasman, *J. Appl. Phys.* **48** (1977) 2692. https://doi.org/10.1063/1.324119